Optimization of electrochemical time of flight measurements for precise determinations of diffusion coefficients over a wide range in various media

Jonathan Moldenhauer, Catherine Sella, Becca Moffett, Joel Baker, Laurent Thouin, Christian Amatore, Stefan Kilyanek, David Paul

▶ **To cite this version:**

Jonathan Moldenhauer, Catherine Sella, Becca Moffett, Joel Baker, Laurent Thouin, et al.. Optimization of electrochemical time of flight measurements for precise determinations of diffusion coefficients over a wide range in various media. Electrochimica Acta, 2020, 345, pp.136113. 10.1016/j.electacta.2020.136113 . hal-02565765

HAL Id: hal-02565765
https://hal.science/hal-02565765

Submitted on 7 Nov 2020

HAL is a multi-disciplinary open access archive for the deposit and dissemination of scientific research documents, whether they are published or not. The documents may come from teaching and research institutions in France or abroad, or from public or private research centers.

L'archive ouverte pluridisciplinaire **HAL**, est destinée au dépôt et à la diffusion de documents scientifiques de niveau recherche, publiés ou non, émanant des établissements d'enseignement et de recherche français ou étrangers, des laboratoires publics ou privés.

Optimization of Electrochemical Time of Flight Measurements for Precise Determinations of Diffusion Coefficients over a Wide Range in Various Media

Jonathan Moldenhauer [a], Catherine Sella [b], Becca Moffett [a], Joel Baker [a], Laurent Thouin [b]*, Christian Amatore [b,c], Stefan M. Kilyanek [a], and David W. Paul [a]

[a] *Department of Chemistry and Biochemistry, University of Arkansas, 1 University of Arkansas, Fayetteville, AR 72701, USA*

[b] *PASTEUR, Département de chimie, École normale supérieure, PSL University, Sorbonne Université, CNRS, 75005 Paris, France*

[c] *State Key Laboratory of Physical Chemistry of Solid Surfaces, Department of Chemistry and Chemical Engineering, Xiamen University, Xiamen, 361005 China*

Abstract: Diffusion coefficients are an important physical property to both physical and analytical electrochemistry and the role they play in sensors, batteries, and catalysis. In electrochemical time of flight (ETOF), the time needed for an electrochemically generated species to travel to an adjacent electrode is measured. Previously relegated to verifying diffusion modeling and theoretical work, ETOF is a powerful and elegant technique whose broad applicability has been overlooked. In the determination of diffusion coefficients, ETOF does not require setting delicate hydrodynamic conditions required by rotating ring disk (RDE) methods. In addition, no foreknowledge about the complete electrochemical mechanistic system, nor about its electron stoichiometry is required. ETOF is ideal for determining the diffusion coefficients for non-elucidated systems, such as for short-lived intermediates assuming they survive ETOF travel time. Here we report the construction of an empirical calibration curve for the determination of diffusion coefficients using experimental parameters optimized by computer modeling. Using a platinum micro electrode array, diffusion coefficients were determined for a variety of species including ferrocenium, ruthenium(III) bisbipyridine dichloride, and vanadium(III) acetylacetonate, some of which being previously unreported. The elegance of the method is that the calibration curve constructed with a few well-established species in a given electrolyte can be used for any species in any electrolyte.

Keywords: Electrochemical time-of-flight, Diffusion coefficient, Generator-collector mode, Calibration curve, vanadium(III) acetylacetonate

1. Introduction

In addition to being a fundamental property of any solute, diffusion coefficient values are crucial in several applications of electrochemistry. Diffusion plays a pivotal role in analytical or mechanistic investigations as well as for amperometric and potentiometric sensors(1), electrosynthesis(2), redox flow batteries(3), etc. These are all applications where the electrical response depends on the diffusion of molecules to and from an electrode. Typically, precise diffusion coefficients values, *D*, are determined either by electrochemical means using for example scanning electrochemical microscopy (SECM) (4-9) or rotating ring disk (RDE) methods (10-17). RDE methods are based on the Levich equation, Eq 1. The RDE limiting diffusion current plateau value, i_{Lev}, is directly proportional to the two-thirds root of diffusion coefficient of the analyte, *D.* However, prior knowledge of the number of electrons transferred, *n*, the active area of the electrode, *A*, the kinematic viscosity of the supporting electrolyte, ν, and the analyte concentration of the bulk solution, C_s (12) is also required. To determine the diffusion coefficients i_{Lev} values are plotted as a function of $\sqrt{\omega}$. The slope is determined and D is calculated.

$$i_{\mathrm{Lev}} = 0.620nFAD^{\frac{2}{3}}\omega^{\frac{1}{2}}\nu^{\frac{-1}{6}}C_s \quad (1)$$

This can lead to experimental challenges, as several of the terms in the slope of Eq. 1 must be known to calculate the diffusion coefficients. Due to specific mechanistic circumstances, *n* may not be an exact integer (18) since it may vary continuously with the timescale of the experiment(19). Kinematic viscosity of the solution and the concentration of the analyte can be determined through additional experiments, but this makes for an additional burden. In addition, every electroactive analyte experiences different diffusion

58 coefficient values in different media. Using RDE to determine diffusion coefficients
59 requires a new Levich plot to be constructed for each Red/Ox analyte every time any of
60 the terms n, A, ν, and C_s change. Finally, it should be noted that Eq. 1 relates to the
61 diffusion coefficient of the bulk electroactive species in solution and not the product(s)
62 formed by reduction or oxidation. Diffusion coefficients of reaction products can be
63 measured by RRDE, but that technique is not used routinely for this purpose.

64 It is also possible to determine values of n and D simultaneously by comparing responses
65 from a transient technique to that of a steady state technique at a microelectrode.
66 However, in order to avoid biases introduced by the exact electrode surface area and
67 size, the method requires the use of an internal standard with known n and D. The
68 techniques also requires high experimental precision and accuracy. In addition, when n
69 values are susceptible to depend on the time scale due to kinetics special care is required
70 to compare responses corresponding to the same time-scale as detailed in reference(18).

71 In SECM, the probe serves as the detecting electrode for a redox species generated at
72 the surface under examination. The diffusion coefficient is determined by measuring the
73 time of maximum collection at different probe distances from the surface. In this respect,
74 SECM and electrochemical time of flight (ETOF) (20) are formally identical as both involve
75 generation and collection of the species of interest. SECM and ETOF approaches differ
76 only in that SECM relies on collector-generator current feedback magnitude (viz., on
77 collection efficiencies), while ETOF relies on direct measurements of travel times of the
78 generated species of interest between its source (the generator electrode) and its sink
79 (the collector electrode(s)(21). Additionally, SECM-based methods may not be applicable

in structured electrolyte media such as polymers or sol-gel materials in which diffusion coefficient values may be required (17).

1.1 ETOF principle

ETOF is a well established method, first developed by Royce Murray(22) to determine diffusion coefficients. In this work we wish to introduce a new and universal application of its principle to measure diffusion coefficients in any medium and electrolyte based on reference measurements made in another one. For this reason let us first recall the principle and theoretical basis of ETOF to allow the introduction of its present application.

ETOF consists in measuring the time that a generated species took to travel from one electrode to an adjacent detecting electrode; the travel time could then be related to the diffusion coefficient. Murray was interested in determining the apparent diffusion coefficients of electron-hopping across conducting polymers sandwiched between two electrodes. For ETOF travel time of maximum collection, t_{mc}, relates the diffusion coefficient, D, through Einstein's equation, (Eq. 2), to the distance traveled or gap, g, between the two electrodes and a numerical dimensionless constant, K, that depends exclusively on the electrode array geometry. The latter does not depend on the electrochemical medium, nor on the half-life time, $t_{1/2}$, of the species of interest provided that $t_{1/2}$ is greater than t_{mc}.

$$g = K\sqrt{D t_{mc}} \qquad (2)$$

K can be predicted computationally for generator-collector systems having ideal geometries (23, 24) or evaluated empirically based on calibrations performed for micro-systems of any geometry (25-27). In the most popular procedure of ETOF, the generator

is pulsed to a potential that generates a swarm of diffusible species, while the detector is held at a constant potential in order to re-reduce or re-oxidize the generated species (Fig. 1A). These experiments have been limited to model compounds such as ruthenium hexamine(24, 26), ferricyanide(23, 24), hydroxymethylferrocenium(28) or the analyte of interest in a previous study(25). Most of the literature reports the use of ETOF as a way to verify computational models of diffusion between electrodes, viz., as a way to assess experimentally the "ideality" of the microfabricated electrode pattern. The current ETOF approach has been to measure t_{mc} at various distances between the generating and detecting electrodes to determine diffusion coefficients, and then compare to the theoretical estimate. Here we point out that the practical applications of ETOF have been largely over looked, and ETOF is a simple technique capable of measuring the diffusion coefficients of a variety of substances in various media.

1.2 Previous Work and Outline of this Work

Previously some of us presented a novel data treatment for ETOF that provided a simple and elegant method for determining diffusion coefficients(29). In this approach, a calibration curve is constructed by measuring the time of maximum collection (t_{mc}) between two parallel band electrodes in a microelectrode array of having a single and constant distance, g, between the generator and collector electrodes. Using species with known diffusion coefficients as "standards" in the medium of interest, t_{mc} is recorded for each electrochemically generated species. Rewriting Eq. 2 as

$$\sqrt{t_{mc}} = \frac{g}{K\sqrt{D}} \tag{3}$$

123 and plotting $\sqrt{t_{mc}}$ variations as a function of $\frac{1}{\sqrt{D}}$ produces a calibration curve that is used
124 to determine diffusion coefficients of unknown species regardless of other characteristics
125 of the medium and of the species.

126 In this paper, we have expanded electrolyte solutions to include non-aqueous solvents.
127 In addition, computer modeling assisted the optimization of the pulse widths for the
128 generator so that diffusion coefficients could be determined over a large dynamic range
129 with an adequate precision and accuracy.

130 **2. Theoretical optimization of precision and accuracy in ETOF measurements**

131 As shown in Fig. 1, applying a sufficiently brief potential pulse to the generator electrode
132 generates a local concentration of B in its immediate vicinity(30). Diffusional broadening
133 of this concentration pulse over the insulating gap *g* allows capture by the collector(s);
134 because of the short duration of the generator pulse, B is rapidly exhausted. Hence, a
135 peak-shaped current response is expected at the collector (23, 31) whose maximum time
136 position, t_{mc}, in a static solution is directly correlated to the time-of-flight (TOF) of species
137 B. However, if the pulse width (t_{pulse}) is too long, and the electrochemical detection of B
138 regenerates A at the collector electrode, the regenerated species A may then diffuse back
139 to the generator electrode where it can again form B. This redox-cycling leads to an
140 inaccurate value for *D*. Specifically, the result of redox-cycling is that the time position of
141 the maximum collector current t_{mc} shifts towards greater values since it now represents a
142 convolution between the shortest TOF and the maximum redox-cycling efficiency. In the
143 absence of any noise or background interference, a t_{pulse} value preventing redox-cycling
144 gives the most accurate values for *D* of species B. At the other extreme, too short t_{pulse}

145 values lead to generating small quantities of B which are difficult to detect with proper
146 precision at the collector, lowering the accuracy of t_{mc} determination. This experimental
147 conflict between accuracy and precision indicates that the t_{pulse} value should be
148 maximized, yet less than t_{pulse}^{max}, the value beyond which redox-cycling contributions will
149 alter the accuracy. Modeling the diffusion demonstrates that the t_{pulse}^{max} value is not
150 universal but depends on the rate of diffusion of the species of interest over the insulating
151 gaps. However, even an unknown diffusion coefficient can be approximated by simple
152 measurements of t_{mc}.

153 The present work shows that modeling can guide the selection of experimental
154 parameters for ETOF resulting in the accurate determination diffusion coefficients, as well
155 as further validating the experimental principle of determining diffusion coefficients by
156 ETOF. Because *K* and *g* are geometric parameters, independent of the properties of the
157 electrolyte medium and of the substrate whose *D* value is sought to be measured, it is
158 possible to construct an empirical calibration curve relating *D* and t_{mc} values (Eq. 3) using
159 a series of parallel microelectrode arrays. Once the calibration curve is constructed in one
160 medium, the same microelectrode array (with the same geometry) may then be used to
161 determine diffusion coefficients of other species in any media. One can measure the t_{mc}
162 value of an electrogenerated species in any medium, and take that t_{mc} to the calibration
163 curve and estimate the *D* for that species in electrolyte medium used. There is one caveat.
164 Since the diffusion coefficient for a species may vary greatly from one medium to the next,
165 t_{pulse}^{max} along with t_{mc} may vary, leading to an inaccuracy in the determination of diffusion
166 coefficient caused by redox-cycling (*vida supra*). For these reasons, we wish to present

the results of a simplified theoretical analysis aimed to evaluate the relationship between $t_{\mathrm{pulse}}^{\max}$ and t_{mc} values.

2.1 Numerical Simulations using COMSOL

Our theoretical analysis was performed using COMSOL simulations of ideal micro-device systems consisting of three parallel microband electrodes of common width, *w*, separated by insulating gaps of common width *g* with the array being imbedded flat in an insulating plane (Fig. 1A)(20, 29). Owing to its scope, this theoretical analysis was simplified assuming that the electrodes present no vertical edges and that no metallic conductor was located within the gap separating the generator and collector electrodes in order to avoid complications related to any bipolar activity that may be induced over such isolated conductors(32, 33).

We assume that the semi-infinite bulk electrolyte contains only species A. Species A reduces or oxidizes at the generator electrode whose potential is stepped for a fixed time duration, t_{pulse}, and then returned to an open circuit potential (Fig. 1B). This generates a peak-shaped current response (Fig. 1C) characterized by its current maximum, i_{mc}, and its time position, t_{mc}, after the beginning of the pulse (t = 0).

Fig. 2A illustrates the outcome of the corresponding simulations showing how the collector peak-shaped response varies when t_{pulse} increases. Fig. 2B reports the variations of t_{mc} normalized to its ideal limit when $t_{\mathrm{pulse}} \rightarrow 0$, as a function of t_{pulse} also normalized to the same limit. The dimensionless presentation of the theoretical results in Fig. 2B is independent of the exact nature of the redox system considered and of the geometry of device used, provided that the width, *w*, of the band electrodes remains

sufficiently small vs the gap, *g*. The results in Fig. 2B evidence that t_{pulse}/t_{mc} must be smaller than 0.03~0.04 to yield accurate measurements. This constraint is independent from the exact mechanism involved by the electrochemical processes investigated provided that the species B generated at the generator by reduction or oxidation of species A is the only one that is collected at the collector. In the case here, the generator and collector potentials are experimentally chosen so that the reduction of A (or its oxidation) and the detection of B are performed at the current limiting plateaus of the corresponding electrochemical waves. B could be a follow-up product resulting from an EC mechanism at the generating electrode, e.g.: A +/- $e^- \rightarrow A^{\pm} \rightarrow$B. One constraint is that the half-life time, $t_{1/2}$ of $A^{\pm}$, the primary intermediate formed by the reduction of A, must be negligible compared to t_{mc}. If that were not the case, the ETOF method would provide a "mixed" diffusion coefficient convoluting those of B and $A^{\pm}$. Therefore, the ETOF method should be reserved for the analysis of redox systems whose CV simultaneously displays the voltammetric waves of A (forward scan) and B (backward scan) containing no intermediate wave within a single voltammetric scan. The time scale is such that the scan rate, v_{mc}, should be approximately $v_{mc} \sim RT/(Ft_{mc})$ where *R* is the gas constant, *F* is the Faraday value, and *T* is the absolute temperature(34). As discussed later we discovered such a case when determining the diffusion coefficient for the oxidation product of $VO(acac)_2$. (*vida infra*) whose oxidation has been reported to provide a chemical conversion to $V(acac)_3$.(35).

2.2 Conclusions from Simulations with COMSOL

The first conclusion of this theoretical analysis is that the duration of the generator pulse duration, t_{pulse}, should not exceed a maximum value being ca. 0.03 to 0.04 times that of

212 the minimal value of the experimentally determined t_{mc}. This is especially important when
213 dealing with an unknown system. t_{mc} can be evaluated from several experiments at
214 different t_{pulse} to respect the criterion in Fig. 2B. A second conclusion is that the ETOF can
215 determine the diffusion coefficient of any species that is the product of the reduction or
216 oxidation of a precursor species, A or a chemical product from an EC mechanism
217 provided the $t_{1/2}$ of its formation from the primary generated product is negligible vs t_{mc}.

218 **3. Experimental**

219 *3.1 Materials and electrochemical device*

220 All electrochemical measurements were performed using a CHInstruments 750a
221 bipotentiostat. The time duration and application of t_{pulse} for the generator was controlled
222 by National Instruments LabVIEW software. Microband electrode arrays of 16 platinum
223 or gold fingers, 2 mm long, 25 μm wide with gaps of 25 μm were fabricated at the
224 Arkansas High Density Electronics Center (HiDEC). Using either one of these arrays
225 provided essentially identical results. A saturated KCl Ag/AgCl reference electrode was
226 used in aqueous solutions. A saturated calomel electrode fitted with an organic solvent
227 bridge made with $TBAPF_6$ in the solvent considered was constructed for use in organic
228 solvents. Measurements were performed in a VAC-atmospheres glovebox with a purified
229 anhydrous nitrogen atmosphere. The atmosphere was purged extensively between
230 experiments while the SCE was sealed in a gastight container.

231 *3.2 Chemicals*

232 Diffusional reference “standards”, potassium ferrocyanide (Certified ACS grade, Fischer),
233 potassium ferricyanide (Certified ACS grade, Fischer), ruthenium (III) hexamine chloride

(Alfa Aesar), ferrocene (98% Sigma Aldrich), ferrocene acetic acid (98% Sigma Aldrich), and ruthenium bisbipyridine dichloride ($Ru(bpy)_2Cl_2$) (97% Sigma Aldrich) were used as received. Two electrolyte solutions were made: one (aqueous) consisting of 0.1 M KCl (ACS grade, J.T. Baker); the other (organic) consisting of 0.1 M $TBAPF_6$ (98%, Sigma Aldrich) in acetonitrile (HPLC Grade, Fischer). The vanadyl acetylacetonate ($VO(acac)_2$) was synthesized from Vanadium(V) Oxide (98%, Sigma Aldrich) and acetylacetone (Reagent Plus grade, Sigma Aldrich) according to the literature method and was recrystallized from dichloromethane (36).

3.3 Conditions of electrochemical measurements

5 mM solutions were made of each "reference" electroactive compound, i.e. those with known diffusion coefficients. Three equally spaced (gap distance of g=75μm) microband electrodes (w=25μm) were selected by pairing sets of microbands available in the microfabricated arrays to perform ETOF measurements. The other 13 microbands present in the array were left open-circuit. The generator electrode potential was imposed for a time duration, t_{pulse}, and then open circuited to minimize current feedback. The potentials on the two flanking collector electrodes remained continuously poised(29).

The applied potentials values were determined using cyclic voltammetry (CV). CV was also used to ensure that the condition $t_{1/2} << t_{mc}$ was valid for complex mechanisms. Measurements were performed in either 0.1 M KCl or in 0.1 M $TBAPF_6$ / acetonitrile. For the latter case, unless otherwise noted, all potentials were referenced to a SCE using a double salt bridge. The potential window for the CV for ferrocene and ferrocenyl acetic acid solutions was from -0.6 V to +0.8 V, and the ETOF potentials were selected as

follows. For experiments with ferrocene, the generator was pulsed to +0.8 V while the collectors were held at +0.1 V. For ferrocene acetic acid, the generator was pulsed to +0.5 V while the collectors were held at +0.1 V. The CV potential window for $Ru(II)(bpy)_2Cl_2$ was +0.5 V to -0.2 V and the ETOF potentials were set at +0.5 V for the generator pulse and -0.1 V for the collectors. The ferrocene/ferrocenium had a known diffusion coefficient in the literature(37) and $Ru(II)(bpy)_2Cl_2$ was compared to an estimated diffusion based on its mass(38).

The mechanism occurring during the $V^{IV}O(acac)_2$ oxidation wave is complex (34,35), possibly leading to formation of $V(acac)_3$ (see Appendix A). The potential window for the CV of $VO(acac)_2$ was thus extended from +2.0 V to -2.0 V to identify the ETOF potentials. These were set at +1.0 V for the generator pulse and -1.5 V for the collectors in order to determine the diffusion coefficient of $V(acac)_3$, the suspected product. Under these conditions, only two waves were observed, the oxidation one of $V^{IV}O(acac)_2$ and the reduction one of its oxidation product observed during the backward scan (35)

4. Results and Discussion

4.1 ETOF calibration curve

An experimental ETOF calibration curve (Fig. 3) was constructed with a constant value of t_{pulse} = 61 ms using the same electrode array as before(29). A calibration curve was constructed based on the experimental $\sqrt{t_{mc}}$ values determined in 0.1 M KCl, using three "reference" species, formed at the generator. The respective *D* values taken from literature reports, vis. ferrocyanide (D = 6.5 x 10^{-6} cm^2/s)(24), ferricyanide (D = 7.2 x 10^{-6} cm^2/s)(39), and ruthenium(II) hexamine (D = 7.8 x 10^{-6} cm^2/s)(24). The *K* constant in Eq.

278 3, was determined from the slope (3.23(±0.03) x10^{-3}) of the regression line after forcing
279 the line through the origin in order to comply with the theory. A band separation of g =
280 75μm provided a value for K = 2.32(±0.02). The t_{mc} measured for these three "reference"
281 species using a t_{pulse} = 61 ms, satisfied the criterion (t_{pulse}/t_{mc} = 0.037), developed by the
282 modeling ensuring no recycling and sufficient collection current to determine t_{mc} with
283 precision.

284 Using this calibration curve, the diffusion coefficients values for the other species
285 ferrocenium and ferrocenium acetic acid could be determined based on their t_{mc} values.
286 However, the case of ferrocene/ferrocenium serves to illustrate the danger of using too
287 large a value for t_{pulse}. The ferrocenium generated has a three times larger diffusion
288 coefficient, D = 2.24(±0.07) x10^{-5} cm^2/s (37), than those used to construct the calibration
289 line in Fig. 3. Use of the same pulse width t_{pulse} = 61 ms, resulted in a t_{mc} value of 0.93 s,
290 which the calibration curve translated as a diffusion coefficient for ferrocenium of
291 1.22(±0.03)x10^{-5} cm^2/s, i.e., half the value of 2.24(±0.07)x10^{-5} cm^2/s reported in the
292 literature (37). Ferrocenium diffuses rapidly making t_{pulse}/t_{mc} = 0.065, resulting in recycling,
293 and yielding an incorrect value. We described this result to illustrate the necessity of
294 respecting the criterion in Fig. 2B, i.e., t_{pulse}/t_{mc} < 0.037. t_{pulse} was then decreased from 61
295 ms to 24 ms, and the resulting diffusion coefficient value of 2.4(±0.1)x10^{-5} cm^2/s for
296 ferrocenium , falling within 7% of the reported literature value in acetonitrile. Fig. 3 shows
297 the relative positions of the two corresponding data points for ferrocenium using both
298 values for t_{pulse}. A similar yet inaccurate value was obtained for the diffusion coefficient of
299 ferrocenium acetic acid (not shown). Using t_{pulse} = 61 ms afforded D = 1.10(±0.05) x10^{-5}
300 cm^2/s for ferrocenium acetic acid using the calibration line in Fig. 3, or half the value of

301 the predicted based on its molecular weight(38). In the case of determining the diffusion
302 coefficient for an unknown species, this illustrates the importance of verifying that the
303 t_{pulse}/t_{mc} criterion be satisfied; easily determined as t_{pulse} is selected and t_{mc} is measured.

304 *4.2 Aqueous Diffusion Coefficient Calibration Curves Can Extend to Organic Solvents*

305 The previous calibration curve in Fig. 3 was constructed using literature values for
306 diffusion coefficients (*D*s) and measuring t_{mc} in 0.1 M KCl for each "reference" species.
307 However, the value of the constant *K* is an intrinsic characteristic of the microelectrode
308 array and not of the redox system investigated nor the electrolyte medium used. Hence,
309 the calibration curve in Fig. 3 should be valid in all electrolytes even if the curve was
310 constructed using different redox couples in 0.1M KCl. To test the validity of this
311 prediction, t_{mc} was determined in 0.1 M $TBAPF_6$ / acetonitrile for the oxidation product of
312 ferrocene and $Ru(bpy)_2Cl_2$. The corresponding results are shown in Fig. 4, the dotted
313 regression line being taken from Fig. 3, using 0.1 M KCl electrolyte. Using the t_{mc} values
314 taken in acetonitrile, and the calibration curve constructed using 0.1 M KCl electrolyte,
315 the resulting diffusion coefficients for ferrocenium (37) and $Ru(bpy)_2Cl_2^+$ (38) matched
316 perfectly the literature data for their diffusion coefficients in acetonitrile. This validates our
317 claim that diffusion coefficient calibration curves constructed using a few "reference"
318 species in a given electrolyte can then be used to determine diffusion coefficients in other
319 electrolytes including organic media. As we will note in the next section the ETOF method
320 is not at all restricted to A/B redox systems involving a single reversible electron transfer
321 step but is also applicable to more complex kinetic sequences, as in the case reported
322 for $VO(acac)_2$ (35).

323 *4.3 ETOF Applied to $VO(acac)_2$ in acetonitrile / 0.1 M $TBAPF_6$*

As mentioned in the Experimental section, the electrochemical oxidation of vanadyl acetylacetonate, $VO(acac)_2$ is reported to lead to $V(acac)_3$ (35). The generation of $V(acac)_3$ from $VO(acac)_2$ has been previously studied(35), (40), (41), (42) but a definitive mechanism of reaction following $VO(acac)_2$ oxidation could not be presented. However, the following critical observations were made. 1) The CV reduction wave of the oxidation product of $VO(acac)_2$ and that of $V(acac)_3$ appear to be the same CV. 2) CV reduction of $V(acac)_3$ affords the oxidation wave of $VO(acac)_2$ and 3) the oxidation products of $V(acac)_3$ formed by controlled potential coulometry can re-form $VO(acac)_2$. With these critical observations in hand it is reasonable to conclude that oxidation of $VO(acac)_2$ forms an intermediate that upon some combination of chemical steps and electron transfer from a variety of homogeneous vanadium species likely leads to the formation of $V(acac)_3$ through a complex but pseudo-reversible redox system.

The ETOF method amounts to determining the diffusion coefficient of the species generated at the generator and not of that present in the solution bulk. The $VO(acac)_2$ / $V(acac)_3$ system offered a good opportunity to test the applicability of ETOF when the electron stoichiometry of the electrochemical reaction(s) producing the species of interest (here $V(acac)_3$) is complex and a priori unknown under analytical conditions. Ultimately ETOF determined the diffusion coefficient for the products of reaction to be consistent with previously measured diffusion coefficients for $V(acac)_3$ (3) offering support to the mechanistic proposals of previous studies suggesting the generation of $V(acac)_3$ from $VO(acac)_2$ and vice versa. However, depending on the side products co-generated with $V(acac)_3$, the electron stoichiometry is impossible to ascertain due to the expected involvement of father-son reactions (see Appendix)

The diffusion coefficient of $V(acac)_3$ in acetonitrile with 0.1 M $TBAPF_6$ as the supporting electrolyte was thus deduced experimentally based on the corresponding t_{mc} value using the calibration curve without any hypothesis about its exact nature. This afforded a value of $1.71(\pm0.08)\times10^{-6}$ cm^2/s (Fig. 4). Such value is in total disagreement with the estimated diffusion coefficient based on the molecular weight of its primary oxidation intermediate $V^{V}O(acac)_2^+$. Conversely, a diffusion coefficient has been reported for $V^{III}(acac)_3$ (3), viz., 1.8×10^{-6} cm^2/s, being only 5% greater than the value measured by ETOF. This finding demonstrates the utility and elegance of the ETOF method allowing for the determination of a diffusion coefficient without a complete mechanistic understanding of the reaction occurring and allowing for identification of the products offering further support for a mechanistic proposal.

5. Conclusions

This work shows that ETOF is an elegant, effective, and simple method that easily determines the diffusion coefficient of the product of a redox reaction in any medium and even when the product is formed through a complex and possibly unknown mechanistic sequence. The ETOF approach relies only on the duration of the diffusional transport between a generator electrode where the species of interest is formed and a collector(s) electrode(s) at which it can be detected electrochemically. In contrast to other methods, ETOF does not rely on the electrochemical current intensities measured. This unique advantage of the ETOF approach has been successfully illustrated in the context of vanadyl acetylacetonate, $VO(acac)_2$, oxidation that underwent a complex mechanism with unknown fractional electron stoichiometry.

A second unique advantage of the ETOF method is that the relationship between the

measured time of flights, t_{mc}, and the sought diffusion coefficients, D, are independent of the electrolyte / solvent media in which the ETOF measurements are performed. Instead, ETOF measurements depend exclusively on the geometrical characteristics of the microband electrode array used. The lack of dependence on solvent / electrolyte media has been illustrated by establishing a calibration curve, $\sqrt{t_{mc}} \propto 1/\sqrt{D}$ (Fig. 3), based on the measurements of t_{mc} values in 0.1 M KCl for a series of species whose diffusion coefficients were reported in the literature and validating its use in 0.1 M $TBAPF_6$ / acetonitrile (Fig. 4).

Albeit these are important and unique advantages, it is emphasized that a proper use of the ETOF method requires that the duration, t_{pulse}, of the potential pulse applied to the generator electrode is sufficiently small compared to the experimental time of flight, t_{mc}. This can be ensured experimentally as shown in Fig. 2B, since for a given species using too large t_{pulse} / t_{mc} values produces an increasing drift of t_{mc} values. Numerical modeling with COMSOL, was especially useful in establishing quantitatively the criterion fixing the upper limit of t_{pulse} values for a given experimental value of the time-of-flight t_{mc}

Acknowledgements

In Fayetteville, this work was supported by the Arkansas Applied Biosciences Institute and the National Science Foundation (CHE-1263119/REU). SMK acknowledges funding from the National Science Foundation (CHE-1654553). In Paris, this work was supported by in parts by Ecole Normale Supérieure, PSL Research University, CNRS (UMR8640), and Sorbonne University. J.M. specially thanks Professor Ingrid Fritsch for helpful

392 discussions and also Nandita Halder & Errol Porter for the fabrication of microelectrode
393 arrays. C.A. thanks the University of Xiamen, China, for his Distinguished Scientist
394 position.

395

396

397

398

399 **Appendix A**

400 The electron stoichiometry of $V^{IV}O(acac)_2$ oxidation at the generator electrode is expected
401 to generate the cation $V^{V}O(acac)_2^+$ as the primary intermediate. The oxidation numbers
402 of the vanadium center are noted in the following to help in recognizing father-son
403 sequences:

404 $V^{IV}O(acac)_2 \leftrightarrow V^{V}O(acac)_2^+ + e^-$ *(expected but not seen)* (A.1)

405 The chemical instability of this primary intermediate was confirmed by the absence of a
406 reduction wave for $V^{V}O(acac)_2^+$ in the CV (Eq. A1). Owing to the reported instability of
407 $V^{IV}O(acac)_2$ (35), $V^{V}O(acac)_2^+$ is expected to undergo a rapid father-son follow-up
408 mechanism (19) in the presence of adventitious water:

409 $V^{IV}O(acac)_2 + H_2O \leftrightarrow V^{IV}O(OH)(acac). + Hacac$ (A.2)

410 $V^{V}O(acac)_2^+ + Hacac \leftrightarrow V^{V}(acac)_3^{2+} + OH^-$ (A.3)

411 $V^{V}(acac)_3^{2+} + 2\ V^{IV}O(acac)_2 \rightarrow 2\ V^{V}O(acac)_2^+ + V^{III}(acac)_3$ (A.4)

412 Eqs. A1-A4 provide one possible mechanism for the extremely fast formation the neutral
413 $V^{III}(acac)_3$ species whose diffusion over the generator-collector(s) gap would then be
414 measured instead of that of the primary oxidation intermediate $V^{v}O(acac)_2^+$. Note that the
415 overall electron stoichiometry of the mechanism in Eqs. A1-A4 is equal to ¼ electrons
416 since one unreacted $V^{IV}O(acac)_2$ is consumed by the ligand exchange in Eq. A2 and an
417 additional two equivalents of $V^{IV}O(acac)_2$ are consumed in Eq. A4 (see Eq. A5).

418 $V^{IV}O(acac)_2 + ¼\ H_2O \rightarrow ¼\ V^{IV}O(OH)(acac) + ½\ V^{V}O(acac)_2^+ + ¼\ V^{III}(acac)_3 + ¼\ OH^- +$
419 $1/4\ e^-$ (A.5)

420 It is also noteworthy that the proposed mechanism is expected to generate an additional
421 two equivalents of $V^{V}O(acac)_2^+$ that can further react extremely fast with free ligand and
422 generate additional $V^{III}(acac)_3$ near the generator electrode. This global stoichiometry
423 would even be more complex if $V^{IV}O(OH)(acac)$ is oxidizable at the oxidation wave of
424 $V^{V}O(acac)_2$:

425 $V^{IV}O(OH)(acac) \leftrightarrow V^{V}O(OH)(acac)^+ + e^-$ (A.6)

426 as suggested by the absence of a reduction wave that could be ascribed to this species
427 in the CV of the $V^{IV}O(acac)_2$ / $V^{III}(acac)_3$ redox system. This may look unlikely at first
428 glance, however, one expects the resulting $V^{V}O(OH)(acac)^+$ species to react much faster
429 in the presence of adventitious water with the parent $V^{IV}O(acac)_2$ species than
430 $V^{V}O(acac)_2^+$:

431 $V^{V}O(OH)(acac)^+ + 2\ V^{IV}O(acac)_2 + H_2O \rightarrow V^{III}(acac)_3 + 2\ V^{V}O_2^+ + 3OH^-$ (A.7)

432 Eq. A6 may thus displace the oxidation wave of $V^{IV}O(acac)_2$ much before its standard
433 potential (43) so that it may occur before that of $V^{IV}O(acac)_2$. The result is that a

434 complicated sequence of electrochemical and chemical events take place at the potential
435 of the $V^{IV}O(acac)_2$ oxidation wave leading to a variety of unstable species and further
436 convoluting the number of electrons passed per vanadyl unit. In other words, depending
437 on the extent of the conversion in Eqs. A6 and A7, the electron stoichiometry of
438 $V^{IV}O(acac)_2$ is expected to be at least ¼ e^- and possibly ranging to larger values. If one
439 were relying on RDE measurements of $V^{IV}O(acac)_2$ oxidation, using the limiting plateau
440 current in RDE would require a foreknowledge of the value, *n*, the apparent number of
441 electrons exchanged per $V^{IV}O(acac)_2$ that would prevail for the RDE rotation rate in order
442 to determine the diffusion coefficient of the products. Similarly, current feedback
443 measurements in SECM are highly dependent on the ability of $V^{IV}O(acac)_2$ to be
444 quantitatively regenerated by oxidation of $V^{III}(acac)_3$ at the collector which cannot be
445 guaranteed within the short time scales of SECM experiments. Conversely, ETOF
446 measurements rely exclusively on diffusional time durations of the $V^{III}(acac)_3$ species and
447 not at all on current intensities.

448

449

Captions of Figures

Fig. 1: (A) Schematic cross section of the device considered in the ETOF experiments. *g* is the gap distance between the electrodes selected to operate as generator and collector electrodes. These electrodes are indicated by black rectangles embedded in the insulating plane. (B) Schematic time dependence of the potential pulse applied at the generator and of the resulting generator current. (C) Corresponding collector response characterized by a peak-shaped current with its maximum characterized by its current, time coordinates (i_{mc}, t_{mc}). Note that the time scales in (B) and (C) are not identical, that in (C) being compressed vs that in (B).

Fig. 2: Illustration of the influence of t_{pulse} on the relative intensity and time position, t_{mc}, of the collector peak response. (A) Collector current responses for increasing t_{pulse} values as determined numerically for the system in Fig. 1A. t_{mc} tends towards a constant value, independent of t_{pulse} when $t_{pulse} \rightarrow 0$. (B) Variation of the ratio t_{mc} /(t_{mc} at $t_{pulse} \rightarrow 0$) as a function of t_{pulse} /(t_{mc} at $t_{pulse} \rightarrow 0$); note that the abscissa in B is in log scale.

Fig. 3: Calibration curve constructed using ferrocyanide, ferricyanide, and ruthenium (II) hexamine in 0.1 M KCl aqueous solution based on t_{mc} values determined from ETOF experiments using t_{pulse} = 61ms and known diffusion coefficients of the generated species (indicated on the graph). The dotted line represents the equation $\sqrt{t_{mc}}$ = 3.23(±0.03)x10^{-3}/$\sqrt{D_B}$. The incorrect t_{mc} values determined for ferrocenium and ferrocenium acetic acid

471 in acetonitrile using t_{pulse} = 61ms are shown by orange circles while the correct one
472 measured for ferrocenium using t_{pulse} = 24ms is shown by a green point.

473

474 **Fig. 4**: Use of the calibration curve, $\sqrt{t_{mc}}$ = 3.23(±0.03)x10^{-3}/$\sqrt{D_B}$, reported in Fig. 3 in 0.1
475 M KCl to determine diffusion coefficients from t_{mc} values determined in acetonitrile with
476 0.1 M $TBAPF_6$ as the supporting electrolyte for generated species: Ferrocenium,
477 $Ru(bpy_2)Cl_2^+$, and $V(acac)_3$. In order to fulfill the criterion t_{pulse} / t_{mc} < 0.037, t_{pulse} = 24 ms
478 was used for Ferrocenium while t_{pulse} = 61 ms was used for the three other species. Blue
479 circles represent the set of data determined for generated species $Ru(NH_3)_6^{2+}$, $Fe(CN)_6^{3-}$
480 and $Fe(CN)_6^{4-}$ in 0.1 M KCl aqueous solution, while orange circles represent the set of
481 data determined in acetonitrile / 0.1 M $TBAPF_6$.

482

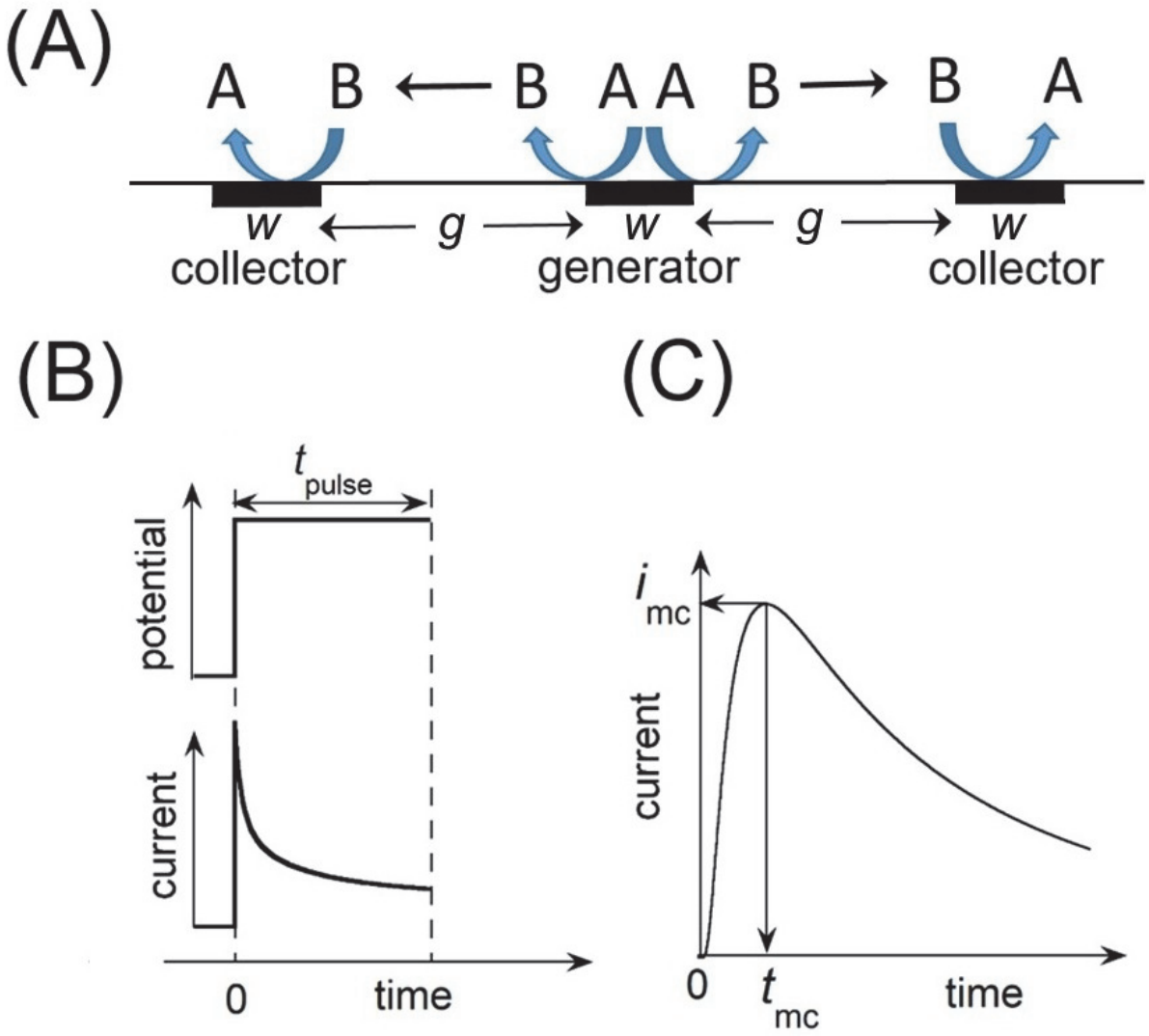

483

484 .

485 **Fig. 1**: (A) Schematic cross section of the device considered in the ETOF experiments. *g*
486 is the gap distance between the electrodes selected to operate as generator and collector
487 electrodes. These electrodes are indicated by black rectangles embedded in the
488 insulating plane. (B) Schematic time dependence of the potential pulse applied at the
489 generator and of the resulting generator current. (C) Corresponding collector response
490 characterized by a peak-shaped current with its maximum characterized by its current,
491 time coordinates (i_{mc}, t_{mc}). Note that the time scales in (B) and (C) are not identical, that
492 in (C) being compressed vs that in (B).

493

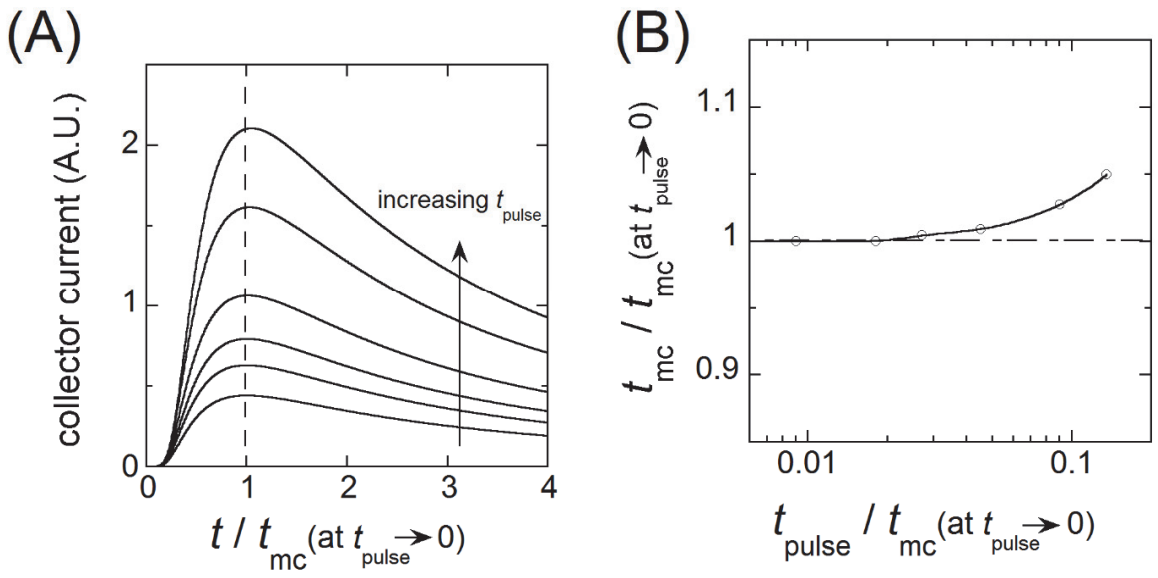

Fig. 2: Illustration of the influence of t_{pulse} on the relative intensity and time position, t_{mc}, of the collector peak response. (A) Collector current responses for increasing t_{pulse} values as determined numerically for the system in Fig. 1A. t_{mc} tends towards a constant value, independent of t_{pulse} when $t_{pulse} \rightarrow 0$. (B) Variation of the ratio t_{mc} /(t_{mc} at $t_{pulse} \rightarrow 0$) as a function of t_{pulse} /(t_{mc} at $t_{pulse} \rightarrow 0$); note that the abscissa in B is in log scale.

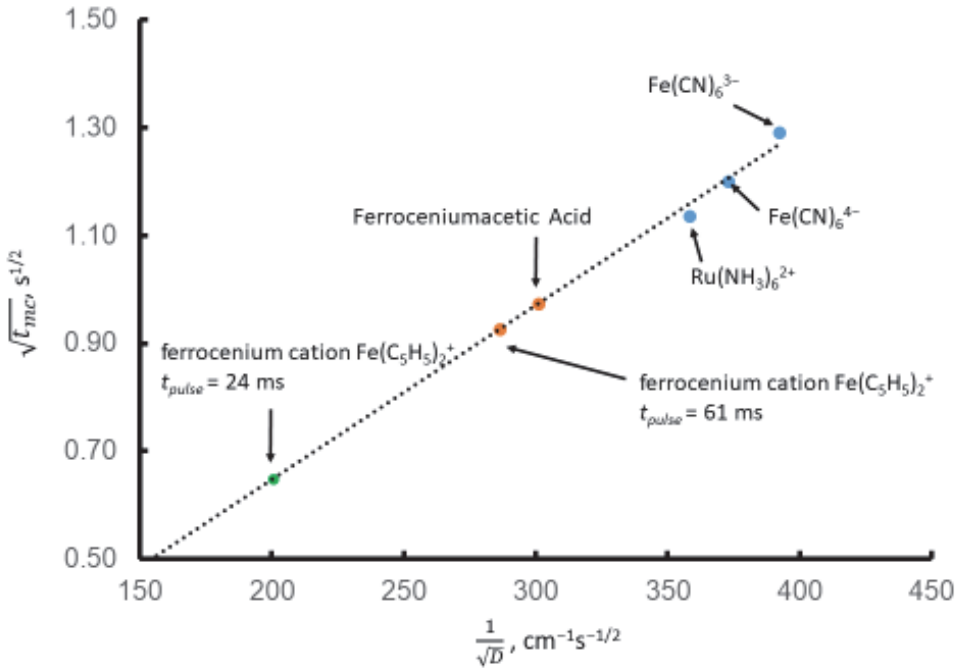

503

504 **Fig. 3**: Calibration curve constructed using ferrocyanide, ferricyanide, and ruthenium (II)
505 hexamine in 0.1 M KCl aqueous solution based on t_{mc} values determined from ETOF
506 experiments using t_{pulse} = 61ms and known diffusion coefficients of the generated species
507 (indicated on the graph). The dotted line represents the equation $\sqrt{t_{mc}}$ = 3.23(±0.03)x10^{-3}/$\sqrt{D_B}$. The incorrect t_{mc} values determined for ferrocenium and ferrocenium acetic acid
509 in acetonitrile using t_{pulse} = 61ms are shown by orange circles while the correct one
510 measured for ferrocenium using t_{pulse} = 24ms is shown by a green point.

511

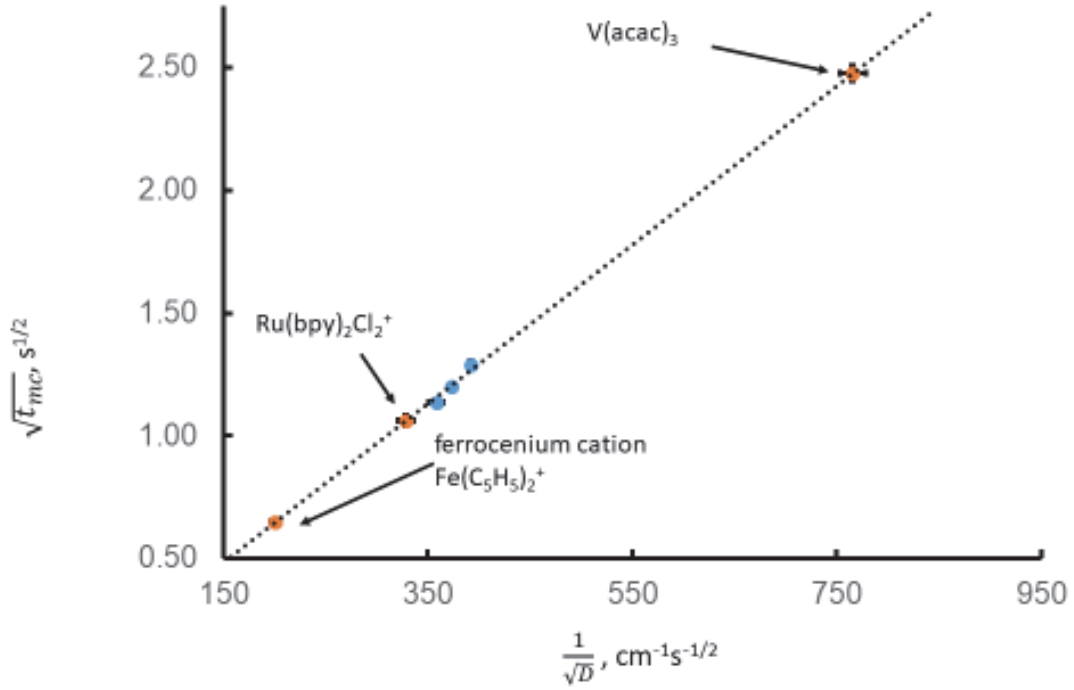

512

513 **Fig. 4**: Use of the calibration curve, $\sqrt{t_{mc}}$ = 3.23(±0.03)x10^{-3}/$\sqrt{D_B}$, reported in Fig. 3 in 0.1
514 M KCl to determine diffusion coefficients from t_{mc} values determined in acetonitrile with
515 0.1 M $TBAPF_6$ as the supporting electrolyte for generated species: Ferrocenium,
516 $Ru(bpy_2)Cl_2^+$, and $V(acac)_3$. In order to fulfill the criterion t_{pulse} / t_{mc} < 0.037, t_{pulse} = 24 ms
517 was used for Ferrocenium while t_{pulse} = 61 ms was used for the three other species. Blue
518 circles represent the set of data determined for generated species $Ru(NH_3)_6^{2+}$, $Fe(CN)_6^{3-}$
519 and $Fe(CN)_6^{4-}$ in 0.1 M KCl aqueous solution, while orange circles represent the set of
520 data determined in acetonitrile / 0.1 M $TBAPF_6$.

521

References

1. C. D. Johnson and D. W. Paul, *Sens. Actuators, B*, **105**, 322 (2005).
2. C. Amatore and J. M. Saveant, *J. Electroanal. Chem. Interfacial Electrochem.*, **126**, 1 (1981).
3. Q. Liu, A. E. S. Sleightholme, A. A. Shinkle, Y. Li and L. T. Thompson, *Electrochem. Commun.*, **11**, 2312 (2009).
4. R. D. Martin and P. R. Unwin, *Anal. Chem.*, **70**, 276 (1998).
5. R. D. Martin and P. R. Unwin, *J. Chem. Soc., Faraday Trans.*, **94**, 753 (1998).
6. R. D. Martin and P. R. Unwin, *J. Electroanal. Chem.*, **439**, 123 (1997).
7. C. G. Zoski, J. C. Aguilar and A. J. Bard, *Anal. Chem.*, **75**, 2959 (2003).
8. C. G. Zoski, B. Liu and A. J. Bard, *Anal. Chem.*, **76**, 3646 (2004).
9. C. G. Zoski, C. R. Luman, J. L. Fernandez and A. J. Bard, *Anal. Chem. (Washington, DC, U. S.)*, **79**, 4957 (2007).
10. G. Che, Z. Li, H. Zhang and C. R. Cabrera, *J. Electroanal. Chem.*, **453**, 9 (1998).
11. A. M. Lehaf, M. D. Moussallem and J. B. Schlenoff, *Langmuir*, **27**, 4756 (2011).
12. T. H. Silva, S. V. P. Barreira, C. Moura and F. Silva, *Port. Electrochim. Acta*, **21**, 281 (2003).
13. R. A. Ghostine and J. B. Schlenoff, *Langmuir*, **27**, 8241 (2011).
14. H. Dong, X. Cao and C. M. Li, *ACS Appl. Mater. Interfaces*, **1**, 1599 (2009).
15. M. Strawski and M. Szklarczyk, *J. Electroanal. Chem.*, **624**, 39 (2008).
16. A. I. Bhatt and R. A. W. Dryfe, *J. Electroanal. Chem.*, **584**, 131 (2005).
17. A. I. Gopalan, K.-P. Lee, K. M. Manesh, P. Santhosh and J. H. Kim, *J. Mol. Catal. A: Chem.*, **256**, 335 (2006).
18. C. Amatore, M. Azzabi, P. Calas, A. Jutand, C. Lefrou and Y. Rollin, *J. Electroanal. Chem. Interfacial Electrochem.*, **288**, 45 (1990).
19. C. Amatore, G. Capobianco, G. Farnia, G. Sandona, J. M. Saveant, M. G. Severin and E. Vianello, *J. Am. Chem. Soc.*, **107**, 1815 (1985).
20. B. Fosset, C. Amatore, J. Bartelt and R. M. Wightman, *Anal. Chem.*, **63**, 1403 (1991).
21. J. Ghilane, C. Lagrost and P. Hapiot, *Anal. Chem. (Washington, DC, U. S.)*, **79**, 7383 (2007).
22. B. J. Feldman, S. W. Feldberg and R. W. Murray, *J. Phys. Chem.*, **91**, 6558 (1987).
23. C. Amatore, C. Sella and L. Thouin, *J. Electroanal. Chem.*, **593**, 194 (2006).
24. S. Licht, V. Cammarata and M. S. Wrighton, *J. Phys. Chem.*, **94**, 6133 (1990).
25. D. Ky, C. K. Liu, C. Marumoto, L. Castaneda and K. Slowinska, *J. Controlled Release*, **112**, 214 (2006).
26. K. Slowinska, M. J. Johnson, M. Wittek, G. Moller and M. Majda, *Proc. - Electrochem. Soc.*, **2001-18**, 130 (2001).
27. K. Slowinska and M. Majda, *J. Solid State Electrochem.*, **8**, 763 (2004).
28. H. B. Tatistcheff, I. Fritsch-Faules and M. S. Wrighton, *J. Phys. Chem.*, **97**, 2732 (1993).
29. J. Moldenhauer, M. Meier and D. W. Paul, *J. Electrochem. Soc.*, **163**, H672 (2016).
30. N. Baltes, L. Thouin, C. Amatore and J. Heinze, *Angew. Chem., Int. Ed.*, **43**, 1431 (2004).
31. C. Amatore, N. Da Mota, C. Sella and L. Thouin, *Anal. Chem. (Washington, DC, U. S.)*, **80**, 4976 (2008).
32. S. E. Fosdick, K. N. Knust, K. Scida and R. M. Crooks, *Angew. Chem., Int. Ed.*, **52**, 10438 (2013).
33. A. Oleinick, J. Yan, B. Mao, I. Svir and C. Amatore, *ChemElectroChem*, **3**, 487 (2016).
34. C. Amatore, Y. Bouret, E. Maisonhaute, J. I. Goldsmith and H. D. Abruna, *ChemPhysChem*, **2**, 130 (2001).
35. M. A. Nawi and T. L. Riechel, *Inorg. Chem.*, **20**, 1974 (1981).
36. A. Vincent, *Educ. Chem.*, **34**, 165 (1997).

37. N. G. Tsierkezos, *J. Solution Chem.*, **36**, 289 (2007).
38. D. P. Valencia and F. J. Gonzalez, *J. Electroanal. Chem.*, **681**, 121 (2012).
39. S. J. Konopka and B. McDuffie, *Anal. Chem.*, **42**, 1741 (1970).
40. M. A. Nawi and T. L. Riechel, *Inorg. Chem.*, **21**, 2268 (1982).
41. J. S. Shamie, C. Liu, L. L. Shaw and V. L. Sprenkle, *ChemSusChem*, **10**, 533 (2017).
42. A. A. Shinkle, A. E. S. Sleightholme, L. D. Griffith, L. T. Thompson and C. W. Monroe, *J. Power Sources*, **206**, 490 (2012).
43. L. Nadjo and J. M. Saveant, *J. Electroanal. Chem. Interfacial Electrochem.*, **48**, 113 (1973).